

2018

Effect of diabetes mellitus on cementum periodontal interface in Streptozotocin-induced diabetic rat model

Medhat Ahmed El-Zainy

Ahmed Mahmoud Halawa

Fatma Adel Saad
Femy1976@gmail.com

Follow this and additional works at: <https://digitalcommons.aaru.edu.jo/fdj>



Part of the [Medicine and Health Sciences Commons](#)

Recommended Citation

El-Zainy, Medhat Ahmed; Halawa, Ahmed Mahmoud; and Saad, Fatma Adel (2018) "Effect of diabetes mellitus on cementum periodontal interface in Streptozotocin-induced diabetic rat model," *Future Dental Journal of Egypt*. Vol. 4 : Iss. 2 , Article 15.

Available at: <https://digitalcommons.aaru.edu.jo/fdj/vol4/iss2/15>

This Article is brought to you for free and open access by Arab Journals Platform. It has been accepted for inclusion in Future Dental Journal of Egypt by an authorized editor. The journal is hosted on [Digital Commons](#), an Elsevier platform. For more information, please contact rakan@aarj.edu.jo, marah@aarj.edu.jo, dr_ahmad@aarj.edu.jo.



Contents lists available at ScienceDirect

Future Dental Journal

journal homepage: www.elsevier.com/locate/fdj

Effect of diabetes mellitus on cementum periodontal interface in Streptozotocin-induced diabetic rat model

Medhat Ahmed El-Zainy^a, Ahmed Mahmoud Halawa^a, Fatma Adel Saad^{b,*}

^a Faculty of Dentistry, Ain Shams University, Egypt

^b Faculty of Dentistry, Future University, Egypt

ARTICLE INFO

Keywords:

Diabetes mellitus
Cementum
Rat
Alveolar bone
Periodontal ligament
Streptozotocin

ABSTRACT

Objective: Diabetes Mellitus is well known to be associated with several oral complications. Thus, this study investigated the effect of diabetes on the cementum-periodontal interface by light and scanning electron microscopy.

Methodology: This investigation was carried out on twenty eight male albino rats weighing from 200 to 220 gm; rats were divided into two groups: group I (control): fourteen animals received intraperitoneal single dose of 1 ml Citrate buffer, group II (diabetic): fourteen animals that were rendered diabetic by intraperitoneal single dose of streptozotocin 40 mg/kg body weight dissolved in 1 ml Citrate buffer and sacrificed 3 weeks after detection of diabetes. Plasma glucose level > 300 mg/dl confirmed diabetes after 3 days. Half of lower jaws specimens were processed for H&E examination by light microscopy of cementum-periodontal interface. From the other half of specimens; extracted mandibular first molars were examined by SEM for changes of cementum surfaces.

Results: Comparing to control group, diabetic rats showed periodontal fibers disorganization and degeneration with loss of Sharpey's fibers attachments. Increased cementoid, resorptive areas of both cementum surface and alveolar bone were evident in addition to the alterations of bone trabeculae.

Conclusions: Diabetes mellitus was associated with variable deleterious effects on periodontium. The histological and scanning electron microscopy changes were most obviously on PDL and least on cementum.

1. Introduction

Cementum is a nonuniform, avascular, not innervated, mineralized connective tissue covers the root dentin and possibly part of the cervical enamel. It serves as an attachment structure for the periodontal ligament [1,2]. Different varieties of cementum were identified in human teeth, the cellular mixed stratified cementum variety in which alternative deposition of acellular extrinsic and cellular intrinsic fiber cementum was not found in rodent molars but is always present in human teeth in both apical and furcation portions [3,4]. The thickness of the cementum layer in healthy subjects is thinnest in the cervical region (20–50 µm) and thickest (150–200 µm) in apical and multirooted furcation regions of teeth [5]. Moreover, Michele et al. [6] stated that cementum exhibits little or no remodelling, but continues to grow in thickness throughout life. It is the adaptable component of periodontium that may respond to functional changes by apposition and patchwise resorption [7]. The morphology of cementum surface in

human teeth was studied by scanning electron microscopy showing that extrinsic Sharpey's fibers occupied almost 100% of acellular cementum surface, about 40% of the surface in cementum with intrinsic fibres but no cells, and 15–40% in cellular cementum. In some regions, no acellular extrinsic fiber cementum could be observed at the very cementum surface [7,8].

Mario et al. [9] described the periodontal ligament (PDL) on light microscope as a band-like fibrous formation connecting radicular cementum with alveolar bone. Furthermore Antonio and Martha [3] added that the cells of periodontal ligament together with the collagen fiber bundles were embedded in the amorphous ground substance. Sharpey's fibers are defined as the collagen fibers of PDL that embedded in cementum and alveolar bone forming an enthesis into both mineralized tissues. The location of Sharpey's fibers is limited to regions closer to the edges of the respective bone and cementum.

It was reported that the genetic, clinical, radiographic and histological aspects of rat periodontium are similar to those of human

Peer review under responsibility of Faculty of Oral & Dental Medicine, Future University.

* Corresponding author.

E-mail address: femy1976@gmail.com (F.A. Saad).

<https://doi.org/10.1016/j.fdj.2018.10.002>

Received 31 August 2018; Accepted 4 October 2018

Available online 09 October 2018

2314-7180/ © 2018 Published by Elsevier B.V. on behalf of Faculty of Oral & Dental Medicine, Future University. This is an open access article under the CC BY-NC-ND license (<http://creativecommons.org/licenses/by-nc-nd/4.0/>).

periodontium [10]. Bjarne [11] reported that rat alveolar bone has a more simple structure than that of human. Haversian systems are numerous in rats but less well developed than in man.

Diabetes mellitus (DM) is a metabolic disease leading to abnormal fat, carbohydrate and protein metabolism. James et al. [12] stated that type I DM is caused by an absolute deficiency of insulin secretion resulting from autoimmune destruction of pancreatic beta-cells (β cells) leading to insufficient production of insulin thus patients are highly susceptible to diabetic ketoacidosis that if untreated can result in coma or death. Lawrence et al. [13] cited that symptoms of marked hyperglycemia (primary feature of diabetes) include polyuria, polydipsia, polyphagia, weight loss and susceptibility to certain infections. The high morbidity and mortality rates in diabetics are associated with microvascular and macrovascular complications as accelerated atherosclerosis.

Zachariasen [14] and Mandel [15] illustrated oral manifestations of diabetics as altered wound healing, increased incidence of infection, xerostomia, sialadenitis, dysgeusia, halitosis, cheilitis, glossodynia and oral ulcers. Likewise, the increased glucose concentration in blood and gingival fluid in diabetics results in classic signs and symptoms of gingivitis and severe periodontitis [16–18]. Therefore Brian [19] and Gokhan et al. [5] added that the risk of PD fibers attachment loss and alveolar bone loss in diabetics was approximately threefold when compared to nondiabetics. Hyun et al. [20] found that the high glucose levels in diabetics impair the capability of periodontal regeneration.

Huafei et al. [21] stated that Streptozotocin-induced diabetes mellitus (STZ-DM) is similar to type I DM in human and exhibits many of DM complications including angiogenesis, diminished growth factor expression and reduced bone formation. As well, Yasuhiro et al. [22] demonstrated extensive alterations in bone and mineral metabolism, significant reduction in parameters for both bone formation and resorption as well as diabetic osteopenia in STZ-induced diabetic mice. Mona et al. [23] added that in STZ-induced diabetic rats, the early stage of DM produced changes in alveolar bone turnover and thus increased the incidence of periodontal disease.

This study aimed to assess the effect of type 1 diabetes mellitus on the cementum-periodontal interface using light and scanning electron microscopy.

2. Materials and methods

2.1. Animals

Twenty eight adult male albino rats weighing from 200 to 220 gm and aged 5–6 months were selected [24] and recorded in “The Medical Research Center”, Faculty of Medicine, Ain Shams University. The animals were housed in wire mesh cages under the optimal experimental conditions; temperature and humidity conditions were controlled as possible during the experimental period. Animals were fed certified pelleted diet and water *ad-libitum*. One week before the experiment, the rats were given an acclimatization period in the experimental unit and their blood sugar and body weight were recorded before the experiment.

Experimental design: The animals were divided into two groups.

Group I (control): Consisted of fourteen animals received a single dose of 1 ml Citrate buffer by intraperitoneal injections. Animals of this group were sacrificed at the same time with animals of gpII.

Group II (Experimental diabetic): Consisted of fourteen animals that were rendered diabetic by intraperitoneal injection of Streptozotocin.

Diabetes induction: The rats were fasted for 14 h and diabetes was induced by an intraperitoneal single injection of 40 mg/kg body weight Streptozotocin (STZ) (Sigma, St. Louis, MO, USA) freshly dissolved in 1 ml Citrate buffer (0.01 M; pH 4.5). After the injection, the animals were given free access to water and food. Blood samples were obtained via vein puncture of the tail under ether anaesthesia. A plasma glucose

level greater than 300 mg/dl confirmed the presence of diabetes that determined 3 days after the drug injection using a glucometer [24].

Three weeks after detection of diabetes, animals of both groups were sacrificed by an intracardiac anesthetic overdose (sodium thiopental 80 mg/kg). The lower jaws of all rats were dissected free and splitted into two halves using surgical scissors. *One half* was processed for routine histological examination by light microscope. From the *other half*, extraction of the first mandibular molar was done and processed for examination by scanning electron microscope. The specimens were rinsed in a water beaker, and then placed in capsules carrying certain codes for each rat.

2.1.1. For light microscopic examination

Jaw specimens were fixed immediately in 10% formaldehyde solution for 72 h. Then, the specimens were decalcified with 10% ethylene diamine tetra-acetic acid (EDTA) solution at 4 °C for about 5 weeks. Then, dehydration in a series of increasing concentrations of alcohol was done followed by alcohol clearance using xylene. Next, the specimens were infiltrated and embedded in paraffin. Sections of 5 μ m thickness were mounted on regular glass slides [25]. Sections were stained by Hematoxyline and Eosin (H&E) for routine histologic examination by research light microscope.

2.1.2. For scanning electron microscopic examination

The extracted mandibular 1st molars from the other jaws halves were fixed immediately in buffered glutaraldehyde (2.5% glutaraldehyde in 0.1 Molar phosphate buffer) pH 7.2, for 2 hs. Then, molars of each group were randomly and equally divided into two samples A, B (7 molars each for groups I and II). **a)** for sample A molars, the roots surfaces were examined immediately in the untreated post extraction condition [26]. **b)** for sample B molars, the roots surfaces were chemically debrided by immersion in 5% sodium hypochlorite at room temperature for 20 minuits [27]. Then all rinsed 2 times in phosphate buffer 15 min for each. Dehydration was then done in a series of increasing concentrations of water/ethanol mixture for 24 hs and 3 times in 100% ethanol for 24hs. Then the specimens were dried in a desiccator for 2hs after that ethanol is substituted by acetone stepwise, the specimens were stored for 24 hrs in acetone concentrates of (80–96%) and 3 times 24 hs in 100%. Dryness in a desiccator for 2 hs was done then by using CO₂ and followed by the vaporization of CO₂ very slowly over a period of 4 hs. Finally, specimens were fixed on a stub and sputtering with 200°A gold layer with an anatech hummer VII sputtering system [28]. Examination of specimens using scanning electron microscope (Philips XL-30) in Anatomy department, Faculty of Medicine, Ain Shams University was done.

3. Results

3.1. Light microscopic results

3.1.1. Group I (control group)

Examination of H&E stained sections of control group showed normal architecture of principal bundles of periodontal ligament including gingival fibers, transseptal ligament & both alveolar crest and horizontal groups of alveolodental ligament. Molar roots dentin was covered by thin acellular extrinsic fiber on the cervical two thirds of the root (Fig. 1). This normal architecture was seen also in oblique & apical groups of the alveolodental. A thicker cellular intrinsic fiber cementum was distributed along the apical third or half of the root. Cementoblasts were seen close to the cellular cementum interposed between PDL fiber bundles. Moreover, Oval spiderlike cementocytes were entrapped in cellular cementum (Fig. 2). Inserting Sharpey's fibers were evident in acellular, cellular cementum and bundle bone. Fibroblasts with their eccentric elongated nuclei arranged in parallel with the direction of the collagen fibers. Bundle bone appeared with well-organized trabeculae of woven and lamellar bone containing few osteocytes. Plump

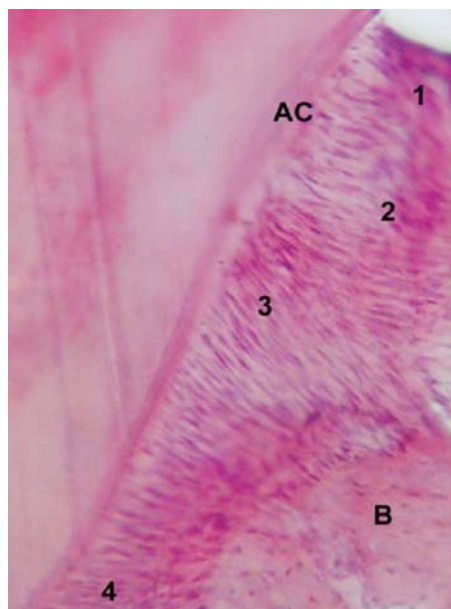


Fig. 1. Photomicrographs of dentoalveolar complex of gpI showing arrangement of periodontal ligament (PDL) fibers and fibroblasts of gingival fibers [1], transseptal ligament [2], alveolar crest gp [3], horizontal gp [4], acellular cementum (AC) and bundle bone (B) (H&E x200).

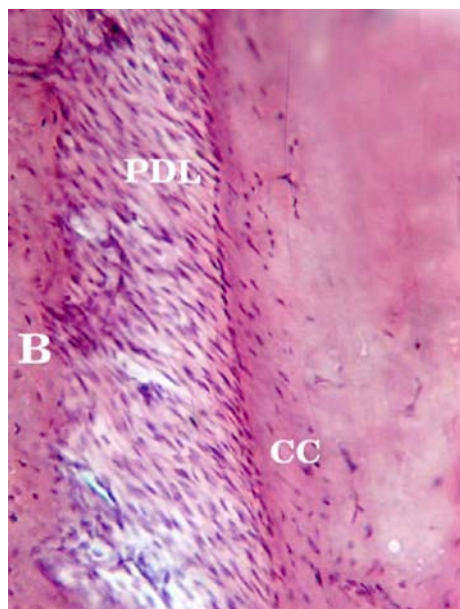


Fig. 2. Photomicrographs of dentoalveolar complex of gpI showing oblique & apical fibers of alveolodental ligament, cellular cementum (CC) and bundle bone (B) (H&E x 200).

osteoblasts bordered alveolar bone trabeculae and marrow spaces (Figs. 1 and 2).

3.1.2. Group II (diabetic)

Streptozotocin-induced diabetic rats compared to control animals; rats lost weight during the 21-days experimental period & were markedly hyperglycemic as blood sugar level ranged from (350–650 mg/dl) compared to control rats as in which it ranged from (92–114 mg/dl).

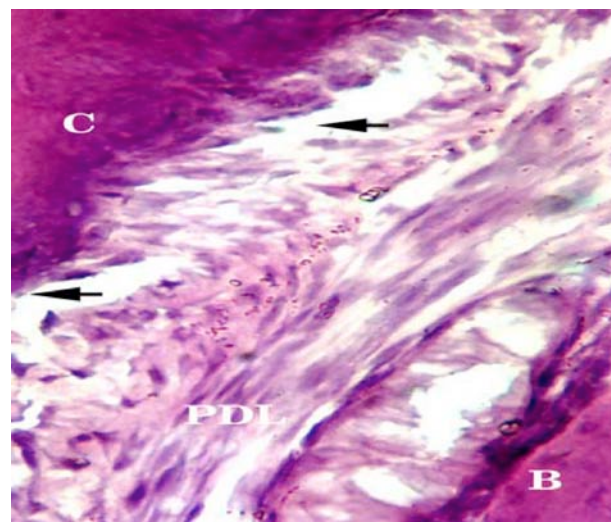


Fig. 3. Photomicrographs of gpII; showing PDL fibers disorganization, degeneration & fibers attachment loss (arrows) (H&E x 400).

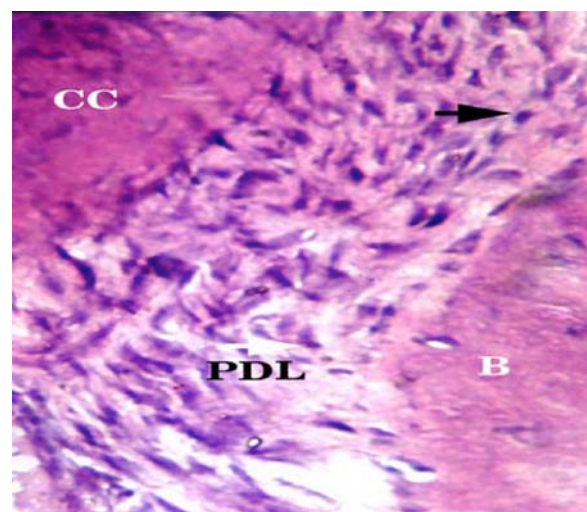


Fig. 4. Photomicrographs of gpII; showing disorientation of periodontal fibroblasts with their elongated intensely stained nuclei & inflammatory cells infiltration (arrow) (H&E x 400).

Examination of Hematoxyline and eosin (H&E) stained sections of gpII demonstrated principle fibers of periodontal ligament thin with wide spaces in some regions. Disorganization and degeneration of the fibers were detected with partly or complete attachment loss of Sharpey's fibers to bone and cementum (Fig. 3). Fibroblasts exhibited disorientation and irregular morphology with shrunken not well delineated intensely stained nuclei. In filtration of inflammatory cells was also observed (Fig. 4). Irregular uneven thickness of mineralized cementum with irregular surface and increased amount of cementoid were noticed (Fig. 5). Cementum surface with reversal line and multinucleated giant cells were detected at the root surface (Fig. 6). Alterations of alveolar bone trabeculae were seen in architecture, thickness and expansion of marrow spaces. Apparent decrease of bone cells (osteoblasts, osteocytes and osteoclasts) with apparent variation in H&E staining reaction of bone matrix was marked. Bone resorption, multinucleated giant cells and reversal lines with Howship's lacunae were also detected at bone surface (Figs. 7 and 8).

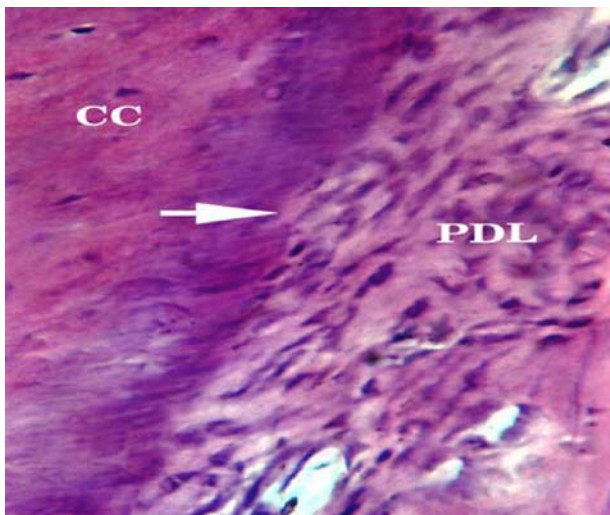


Fig. 5. Photomicrographs of gpII; showing cementum with increased cementoid (white arrow) (H&E x400).

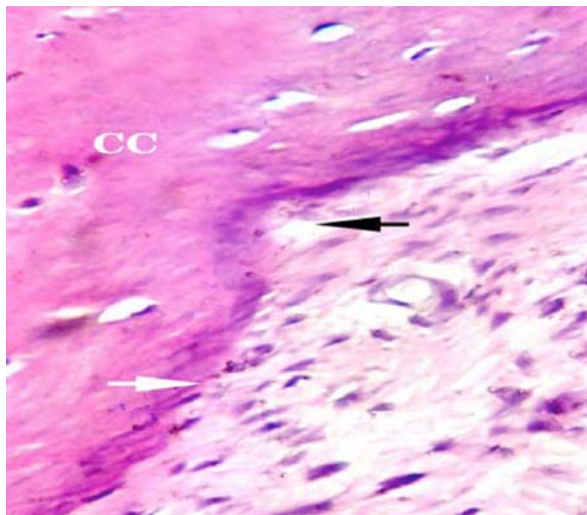


Fig. 6. Photomicrographs of gpII; showing cementum with reversal line (black arrow) (H&E x 400).

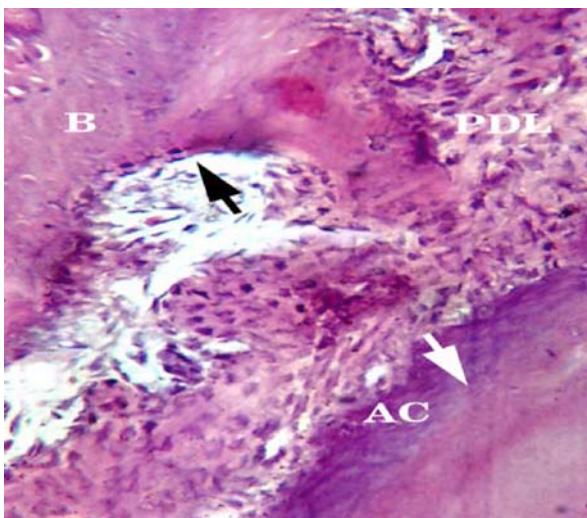


Fig. 7. Photomicrographs of gpII; showing alveolar bone resorption (black arrow) (H&E x 200).

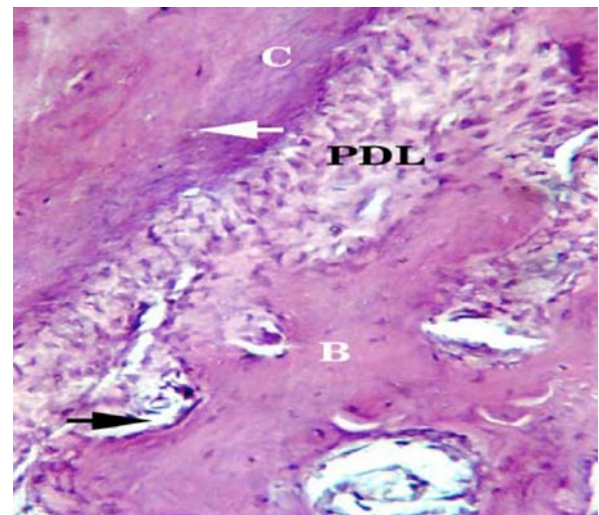


Fig. 8. Photomicrographs of gpII; showing widening of bone marrow spaces, multinucleated giant cells with bone resorption (black arrow) (H&E x 200). PDL: Periodontal ligament, C: Cementum, AC: acellular cementum, CC: Cellular cementum, B: Bundle bone.

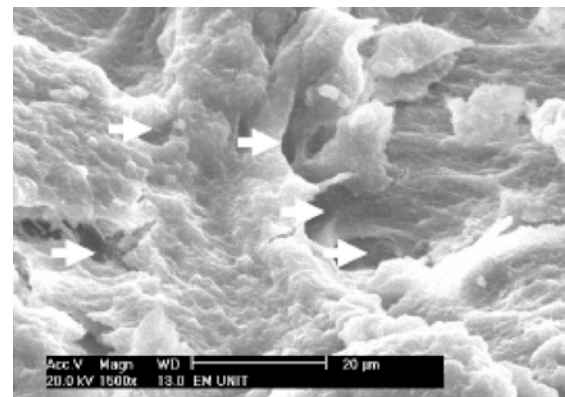


Fig. 9. Scanning electron micrographs of 1st molar untreated root surface of gpI; Cervical third showing cementum surface obliterated by a mat of Sharpey's fibers with empty spaces of cells and blood vessels (arrows) (x1500).

3.2. Scanning electron microscopic results

Examination of root surface of first mandibular rat molar.

3.2.1. Group I (control group)

3.2.1.1. Untreated surfaces in the post extraction condition (sample A). Cervical third: Thick periodontal collagen bundles obliterated the surface of acellular cementum with densely packed and strongly attached Sharpey's fibers to cementum. Spaces for cells and blood vessels were seen among the fibers (Fig. 9).

Apical third: The insertions of the Sharpey's fiber bundles to cementum and the low mound projections of the less densely packed ruptured Sharpey's fibers with varying diameters were observed. Only in very small areas, cellular cementum surface proper could be seen (Fig. 10).

3.2.1.2. Chemical debridement (sample B). Cervical third: SEM of chemically debrided surface of 100% Sharpey's fibers acellular cementum, showed slightly smooth surface with mosaic like appearance (Fig. 11).

Apical third: Cementum surface appeared rough and irregular with dissolved Sharpey's fibers. Holes of disintegrated Sharpey's fibers and cementocytic lacunae were also observed (Fig. 12).

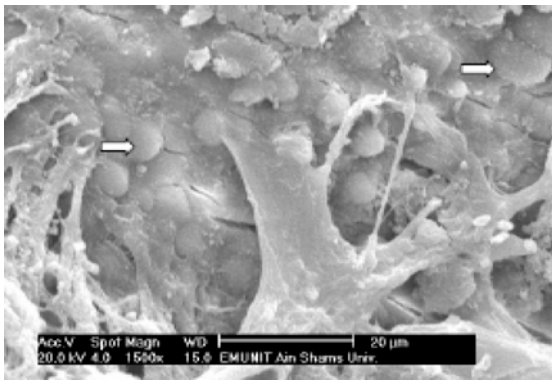


Fig. 10. Scanning electron micrographs of 1st molar untreated root surface of gpI; Apical third showing Sharpey's fiber bundles projecting from cementum and low-mound projections of ruptured Sharpey's fibers (arrows) (x1500).

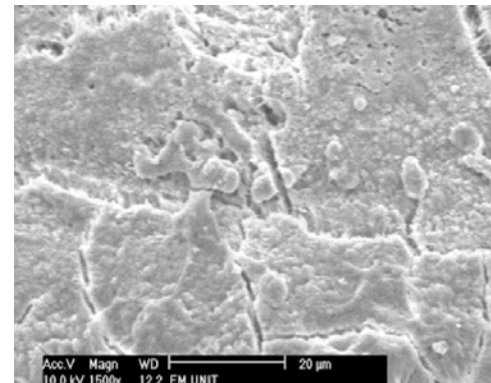


Fig. 13. Scanning electron micrographs of untreated rat 1st molar of gpII; Cervical third showing acellular cementum with irregular areas of cementum proper with no Sharpey's fibers attachment (x1500).

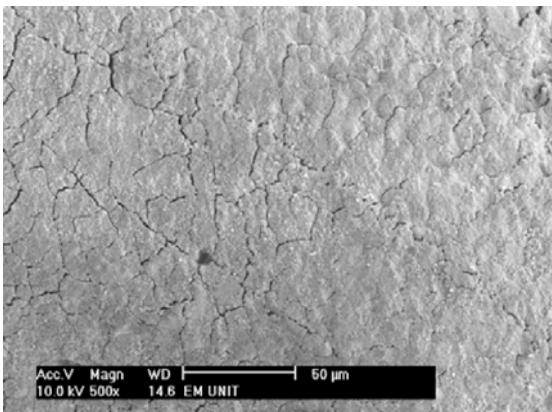


Fig. 11. Scanning electron micrographs of 1st molar root surface after chemical debridement of gpI; Cervical third showing the mosaic like acellular cementum surface regular with narrow cracks (x500).

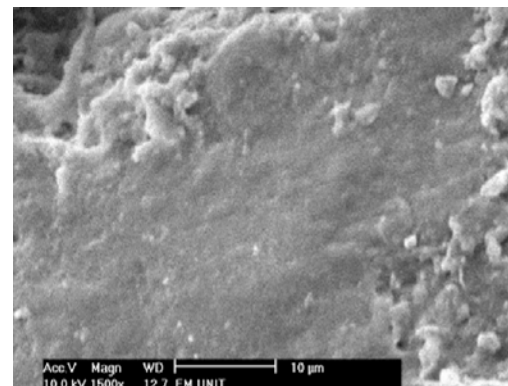


Fig. 14. Scanning electron micrographs of untreated rat 1st molar of gpII; Apical third showing wide area of cellular cementum surface with no fiber attachments (x1500).

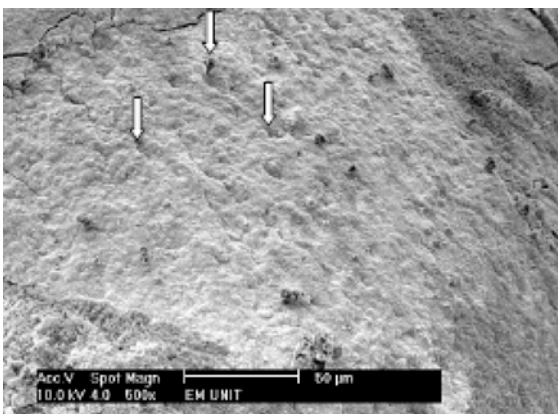


Fig. 12. Scanning electron micrographs of 1st molar root surface after chemical debridement of gpI; Apical third showing cementum surface with narrow cracks, small holes of disintegrated Sharpey's fibers & cementocytic lacunae (arrows) (x500).

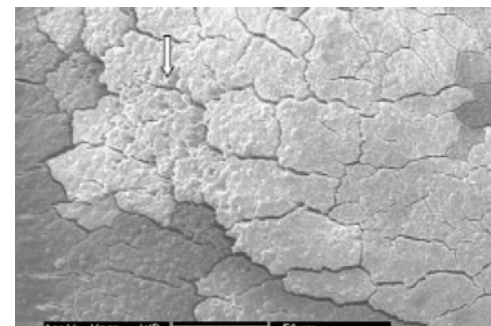


Fig. 15. Scanning electron micrographs of gpII after chemical debridement of rat 1st molar; Cervical third showing acellular cementum surface with changed architecture, wide cracks and pitting in some areas (arrow) (x500).

3.2.2. Group II (diabetic)

3.2.2.1. Untreated surfaces in the post extraction condition (sample A). *Cervical third:* Root surface lost most of its Sharpey's fibers attachment resulted in appearance of areas of cementum proper. Acellular cementum surface with mosaic like pattern showed changed surface architecture and destroyed Sharpey's fibers attachment compared to control gp (Fig. 13).

Apical third: Extensive areas of cellular cementum entirely devoid of penetrating extrinsic Sharpey's fibers were found (Fig. 14).

3.2.2.2. Chemical debridement (sample B). *Cervical third:* Diabetic root surface in mosaic like pattern showed acellular cementum surface with changed architecture, several apparently wide cracks and surface pitting. These resorption pits were seen to be the sites of commencement of repair cellular cementum deposition (Fig. 15). Acellular cementum with several cracks was seen. Badly destructive cementum surface showing multiple shallow and deep resorption bays was observed with loss of cementum characteristic morphology (Fig. 16). Shallow isolated lacuna showed irregularly distributed

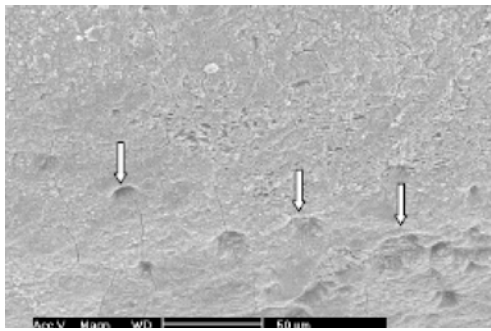


Fig. 16. Scanning electron micrographs of gpII after chemical debridement of rat 1st molar; Cervical third showing cementum surface with cracks and resorption bay's (arrows) (x500).

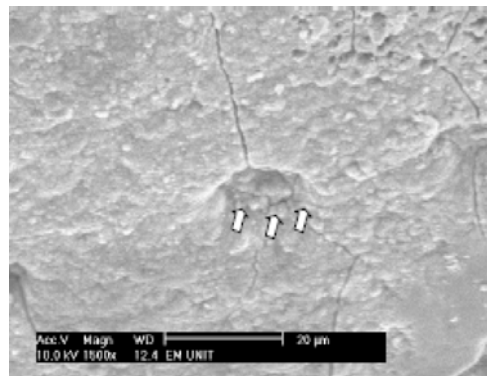


Fig. 17. Scanning electron micrographs of gpII after chemical debridement of rat 1st molar; Higher magnification of resorption bay's filled with repair cementum and disintegrated Sharpey's fibers projections (arrows) (x1500).

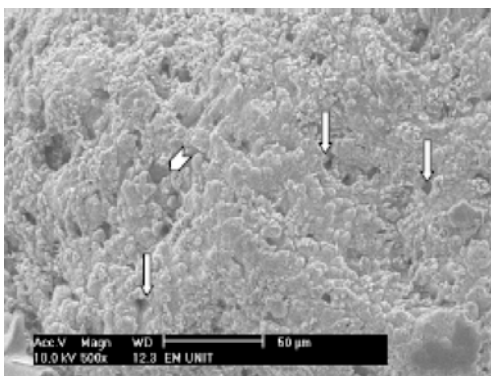


Fig. 18. Scanning electron micrographs of gpII after chemical debridement of rat 1st molar; Apical third showing cementum surface with projections of Sharpey's fibers. Note holes of disintegrated Sharpey's fibers (arrow heads) and cells lacunae (arrows) (x500).

cementum repair at the periphery and the floor of the resorption bay with or without cut Sharpey's fibers projections (Fig. 17).

Apical third: Increased overall roughness of cellular cementum surface was seen by jagged projections of irregular mineralized Sharpey's fibers. Holes of disintegrated Sharpey's fibers and increased cementocytic lacunae were also seen (Fig. 18).

4. Discussion

The cementum-periodontal interface, as a portion of dentoalveolar complex was monitored in this study to detect the alterations caused by DM. Gokhan et al. [5] proved that tooth mobility and loss are among

diabetes complications and occur as a result of periodontitis. In the present study, examination of H&E sections by light microscopy was utilized to show the histological changes of periodontal ligament, cementum (acellular & cellular) and alveolar bone in streptozotocin-induced diabetes mellitus. Herein, SEM was used to examine root surface in untreated post extraction condition [26] to illustrate the relative amount of attached periodontal fibers to cementum (acellular & cellular). Moreover, other samples were chemically debrided before root surface examination [7,29] to remove the non mineralized organic components thus showing the mineralized cementum surface (acellular & cellular).

SEM of untreated samples of control gp showed ruptured Sharpey's fibers in acellular cementum (cervical third) as densely packed low mound projections. While in cellular cementum (apical third) less densely packed Sharpey's fibers projections were seen. These results are coincident with Boyde and Jones [30] who found in human, rats, and some animals that the discrete zones of projections seen by SEM above the plane of cementum mineralization front indicating the distribution of mineralized Sharpey's fibers which mineralized to a level above that of the intrinsic matrix of cementum. Furthermore, SEM results of chemically debrided samples of control gp showed cellular cementum surface (in apical third) with more roughness and irregularities than that of acellular cementum (in cervical third), this could be attributed to the lesser degree of density and mineralization of Sharpey's fibers at cellular cementum surface compared to acellular cementum. These results are in agreement with Jones and Boyde [8] and Schroeder [31] who found that the 100% Sharpey's fibers cementum (acellular cementum) in human presented the inserting fibers with a mineralized center further away from the overall level of cementum surface with about 45–60% overall degree of mineralization. While in 40% Sharpey's fiber cementum (cellular cementum), the fiber was much less mineralized so that overall degree of mineralization is less and is more variable. Moreover, Boyde and Leseter [32] stated that there was an inverse correlation between the degree of mineralization of a calcified collagenous matrix and the manifestation of a fuzzy texture; meaning the tendency of the fibrils to tear out of the plane rather than break cleanly.

Comparing to the control group, routine light microscopic results of diabetic gp revealed disorganization and degeneration of periodontal ligament fibers with infiltration of inflammatory cells. This could be attributed to periodontitis that was described by Sodek [33] who found that the degradation of PDL collagen fibers during inflammation was caused by the release of extracellular collagenolytic enzymes of fibroblasts thus afforded a more rapid and extensive degradation around the cells. Moreover, a decrease in PDL cells that exhibited irregular nuclear morphology as well as the increased inflammatory cells in areas of degenerated PDL fibers were marked in our H&E sections of diabetic gp. Moon, [34] reported that there might be a regulatory mechanism(s) by which PDL fibroblasts maintain their phenotype or differentiate into cementoblasts or osteoblasts. The expression of numerous epidermal growth factor receptors on fibroblasts in functional PDL may be associated with the maintenance of their phenotype as PDL fibroblasts, paravascular cells and pre-osteoblasts. The loss of EGF-Rs is related to the differentiation of these cells into mineralized tissue forming cells. Furthermore, it was found that high glucose concentration level decreased the proliferative capacity of PDL cells and induced resistance to growth factors. Thus, inhibition of PDL cells differentiation and mineralization occurred in high glucose levels [20,35].

In this work, some inflammatory and multinucleated giant cells besides the other periodontal ligament cells were presented in PD areas adjacent to cementum with the loss of fibers attachment to acellular and cellular cementum. Likewise, SEM results of untreated samples (cervical and apical thirds) in diabetic gp ensured H&E results as partial or complete destruction of Sharpey's fibers attachment to cementum was illustrated resulting in appearance of areas of cementum proper. This result is in agreement with Sunita et al. [36] who reported that

5–15 μm wide fibrous region at the root surface has a hygroscopic nature due to the dominance of hydrophilic organic components as glycosaminoglycans, take up water and form stable hydrates [37]. This suggested that this fibrous region may be hypomineralized, making it susceptible to degradation by the inflammatory products due to periodontitis. Furthermore, SEM of chemically debrided samples of diabetic gp revealed badly destructive cementum surfaces with multiple areas of resorption were found particularly in cervical third. Moreover, in some areas, surface pitting was also observed. These findings may be resulted from diabetes associated periodontitis. These results are in agreement with Bilgin et al. [38] who studied by SEM the morphological changes of root cementum layers due to periodontal disease in hopeless extracted teeth and found that presence of cervical root resorption was triggered by the inflammatory process occurred in adjacent connective tissue as a result of periodontitis. Crespo et al. [39] detected histological alterations in root cementum of extracted teeth in different stages of adult periodontitis. The increase in the resorption areas of cementum surface and the severity of periodontal disease that led to more detachment of periodontal ligament fibers were manifested. In disagreement with these findings, Lopez et al. [40] suggested that systemic factors were not an important etiological factor for development of periodontal inflammation and could result from local factors depending on the presence of resorption which would be found in teeth of healthy and unhealthy subjects. In our work, the chemically debrided specimens presented cellular cementum of apical third with Sharpey's fibers projections as flat topped with slit or holes. In coincident with these findings, these projections were described as pointed, jagged mineral fronts of Sharpey's fibers corresponding to the more peripheral parts of the fiber that surrounded an unmineralized core (depression). This indicated that active mineralization proceeded in an irregular fashion [8].

Additionally in this work, histological sections of diabetic gp showed areas of new cementum repair with irregularities of cementum surface. Likewise, the SEM chemically debrided samples showed areas of earlier repair of resorption bays with deposition of new repair cementum at the bays periphery and floor in the cervical third. This new cementum seemed with or without Sharpey's fibers insertions that evidenced by the low mound projections of ruptured fibers at the edges and floor of the bays. These findings are coincident with those of Jones and Boyde [8] who reported that resorption areas appeared to be the nucleus for new cementum formation; cellular cementum containing lacunae and its constituents. It was formed as a response to the need of repairing the resorbed areas that was filled up first with small clusters of mineral particles that usually flowed over on the surrounding unresorbed cementum surface.

Light microscopy of diabetic gp sections showed uneven irregular cementum thickness with increased amount of cementoid on acellular and cellular cementum. In agreement with this result Gokhan et al. [5] stated that irregular thickness of cementum (increase or decrease) can be idiopathic or may result from local factors or could arise from systemic conditions like diabetes. Moreover, Bilgin et al. [38] suggested that the possible mechanism of irregular thickness of diseased cementum was the interruption of continuous cementum deposition during the inflammatory process in the adjacent connective tissue as a result of periodontal disease, while cementum apposition in the healthy parts was continuing.

H&E sections of diabetic gp showed inflammatory cells infiltrates in areas of disintegrated PDL fibers and resorbed alveolar bone as well as alterations in periodontal fibers attachment to alveolar bone. In concurrence with this result, Philip [41] reported that there is a link between poorly controlled diabetic patients and the chronic immune-inflammatory response in which excessive and/or dysregulated local production of inflammatory mediators leads to clinical signs of periodontitis. These signs are characterised by alveolar bone destruction and loss of Sharpey's fibers attachment. As well light microscopy of alveolar bone in diabetic gp showed alterations in architecture and thickness of alveolar bone trabeculae with expansion of marrow spaces.

Areas of bone resorption and Howship's lacunae were also noticed. These results may be attributed to diabetes associated periodontitis. These findings were elucidated with various mechanisms contributed to the pathogenesis of diabetic bone disease and bone abnormalities such as insulin deficiency, hyperglycemia, disturbances in calcium and vitamin D metabolism, chronic malnutrition, microvascular disease of bone and negative bone balance [42,43]. Moreover, Bosshardt [2], Teng [44] and Olszewska et al. [45] stated that normal bone remodelling depends on the delicate balance between bone formation and resorption and associated with RANK/its ligand RANK-L/osteoprotegerin balance. RANK-L and Osteoprotegerin are expressed by stromal cells, PDL fibroblasts and osteoblasts whereas RANK is expressed by osteoclasts precursors. The binding of RANK and RANKL induces osteoclastic differentiation and activity. Osteoprotegerin competes for this binding and functions as natural inhibitor of osteoclasts differentiation and activation. Periodontal infection increases the systemic release of proinflammatory cytokines which can shift the balance towards increased bone resorption. Comparing to control group, diabetic group of our work also manifested apparent decrease of bone cells (osteoblasts, osteocytes and osteoclasts) was observed. Furthermore, bone matrix showed in many areas noticeable variation in H&E staining reaction. This may reflect the variation in the degree of bone mineralization. In clarification of our results, it was evident that normal insulin hormone level exerts direct anabolic effects on bone cells. Insulin directly mediated stimulation of osteoblasts in combination with inhibition of osteoclasts. In diabetes, the inhibition of osteoblastic activity exceeded that of osteoclastic activity. Thus, insulin deficiency in diabetes has a deleterious effect on osseous turnover due to the decrease in osteoblastic and osteoclastic numbers and activities which in turn caused the lower percentage of osteoid surface as well as increased the time for mineralization of osteoid tissue [42,43,46]. Hideki et al. [43] added that decreased bone turnover was thought to result in diabetic osteopenia.

We concluded that diabetes mellitus was associated with variable deleterious effects on periodontium. The histological and scanning electron microscopy changes were most obviously on PDL and least on cementum.

References

- [1] Becker J, Schuppan D, Rabanus JP, Rauch R, Niechoy U, Gelderblom HR. Immunoelectron microscopic localization of collagens type I, V, VI and of procollagen type III in human periodontal ligament and cementum. *J Histochem Cytochem* 1991;39(1):103–10. Jan.
- [2] Bosshardt DD. Are cementoblasts a subpopulation of osteoblasts or a unique phenotype? *J Dent Res* 2005;84:390–406.
- [3] Antonio N, Martha JS. Ten Cate's Oral Histology: development, structure, and function. fifth ed. MI: Mosby-Year Book Inc., St. Louis; 2003. p. 240–74.
- [4] Antonio N, Dieter DB. Structure of periodontal tissues in health and disease. *Periodontology* 2000;40:1–28. 2006.
- [5] Gokhan K, Keklikoglu N, Buyukertan M. The comparison of the thickness of the cementum layer in Type 2 diabetic and non-diabetic patients. *J Contemp Dent Pract* 2004;5(2):124–33. May 15.
- [6] Michele S, Giovanni PP, Massimo C, Alberta L, Gianfranco F. Confocal laser scanning microscopy of human cementocytes: analysis of three-dimensional image reconstruction. *Ann Anat* 2007;189:169–74.
- [7] Iztok S, Gaj V, Erika C, Dominik G. Cementum thickness in multirooted human molars: a histometric study by light microscopy. *Ann Anat* 2008;190:129–39.
- [8] Jones SJ, Boyde A. A study of human root cementum surfaces as prepared for and examined in the scanning electron microscope. *Z. Zellforsch.* 1972;130:318–37.
- [9] Mario R, Claudio C, Viviana DP, Vittoria O, Rita S, Giovanni Z, Alessandro R. A histological and electron-microscopic study of the architecture and ultrastructure of human periodontal tissues. *Arch Oral Biol* 2000;45: 185 \pm 192.
- [10] Page RC, Schroeder E. Periodontitis in man and other animals. Basel: Karger; 1982.
- [11] Bjarne K. Microbiological and immunological aspects of experimental periodontal disease in rats: a review article. *J periodontal* 1991;62:59–73.
- [12] James RG, Alberti KGM, Mayer BD, Ralph AD, Allan D, Steven GG, Saul G, Maureen IH, Richard K, Harry K, William CK, Harold L, Noel KM, Jerry PP, Philip R, Robert AR, Michael PS. Report of the expert committee on the diagnosis and classification of diabetes mellitus. *Diabetes Care* 2003;26:s5–20. January.
- [13] Lawrence C, Tomoya T, Mineko F, Hideto K. Chronic diabetic complications: the body's adaptive response to hyperglycemia gone away? *Trans Am Clin Climatol Assoc* 2006;117:341–52.

- [14] Zachariassen RD. Diabetes mellitus and xerostomia. *Compendium* 1992;13:314–22.
- [15] Mandel ID. Antimicrobial mouthrinses: overview and update. *J Am Dent Assoc* 1994;125(2):2S–10S.
- [16] Finney LS, Finney MO, Gonzalez CJM. What the mouth has to say about diabetes. Careful examinations can avert serious complications. *Review Postgrad. Med* 1997;102(6):117–26. Dec.
- [17] Soskolne WA. Epidemiological and clinical aspects of periodontal diseases in diabetics. *Ann Periodontol* 1998;3:3–12.
- [18] Elter JR, Offenbacher S, Toole JF, Beck JD. Relationship of periodontal disease and edentulism to stroke/TIA. *J Dent Res* 2003;82:998–1001.
- [19] Brian M. tenth ed. Diabetes mellitus. *Burket's in oral medicine (treatment & diagnosis)* vol. 563. 2003. p. 571.
- [20] Hyun SK, Jin WP, Shin IY, Byung JC, Jo YS. Effects of high glucose on cellular activity of periodontal ligament cells in vitro. *Diabetes Res Clin Pract* 2006;74:41–7.
- [21] Huafei L, Douglas K, Louis C, Dana T. Diabetes interferes with the bone formation by affecting the expression of transcription factors that regulate osteoblast differentiation. *Endocrinology* 2003;144:346–52.
- [22] Yasuhiro H, Sohei K, Riko K, Hideki F, Masato K, Masafumi F. Histomorphometric analysis of diabetic osteopenia in streptozotocin-induced diabetic mice: a possible role of oxidative stress. *Bone* 2007;40:1408–14.
- [23] Mona AA, Ippei W, Kunimichi S. The effect of diabetes mellitus on rat mandibular bone formation and microarchitecture. *Eur J Oral Sci* 2010;118(4):364–9. Aug.
- [24] Holzhausen M, Garcia DF, Pepato MT, Marcantonio EJ. The influence of short-term diabetes mellitus and insulin therapy on alveolar bone loss in rats. *J Periodontal Res* 2004;39:188–93.
- [25] Keita M, Noriyuki S, Toru K, Yasuko M, Akihiro H, Hidehiro O. Scanning electron microscopy of the three different types of cementum in the molar teeth of the Guinea pig. *Arch Oral Biol* 2006;51:439–48.
- [26] Adam B, Maria G. Ultrastructural changes of a tooth root in young rats fed a low calcium and vitamin D-deficient diet. *Rocz Akad Med Bialymst* 1997;42(Suppl 2):149–54.
- [27] Jeffrey AC. The use of ultrasound and Sodium Hypochlorite as adjuncts to the cleansing of root canals. *Departement of Operative Dentistry, University Of Sydney*; 1988.
- [28] Ralf J. Preparation of extracted natural human teeth for SEM investigations. *Biomaterials* 1995;16:209–17.
- [29] Safaa AG, Suzi S. Scanning electron microscopic study of root resorption and repair in response to low magnitude of force. *Egypt Orthod J* 2007;31:39–50.
- [30] Boyde A, Jones SJ. Scanning electron microscopy of cementum and Sharpey's fibre bone. *Z. Zellforsch.* 1968;92:536–48.
- [31] Schroeder HE. Biological problems of regenerated cementogenesis: synthesis and attachment of collagenous matrices on growing and established root surfaces. *Int Rev Cytol* 1992;142:1–58.
- [32] Boyde A, Lester KS. An electron microscope study of fractured dentinal surfaces. *Calcif Tissue Res* 1967;1:122–36.
- [33] Sodek J, Overall CM. Matrix degradation in hard and soft connective tissues. In: Davidovitch Z, editor. *Biological mechanisms of tooth eruption and root resorption*. Birmingham: EBSCO Media.; 1988. p. 237–42.
- [34] Moon ILC. Periodontal ligament and cementum. *Adv Dent Res* 1995;9(3):17. November.
- [35] Hehenberger K, Hansson A. High glucose-induced growth factor resistance in human fibroblasts can be reversed by antioxidants and protein kinase C-inhibitors. *Cell Biochem Funct* 1997;15:197–201.
- [36] Sunita PH, Sally JM, Mark IR, Grayson WM. The tooth attachment mechanism defined by structure, chemical composition and mechanical properties of collagen fibers in the periodontium. *Biomaterials* 2007;28:5238–45.
- [37] Arthur RH, Richard AT. *Ten Cate's Oral Histology: development, structure, and function*. fifth ed. St. Louis: MI: Mosby-Year Book Inc.; 1998. p. 73.
- [38] Bilgin E, Gürgan CA, Nejat AM, Bostanci HS, Güven K. Morphological changes in diseased cementum layers: a scanning electron microscopy study. *Calcif Tissue Int* 2004;74:476–85.
- [39] Crespo AAC, Rodríguez CMA, Fuentes BIM, Castaño OMT, Jorge BFJ, Rodríguez PRB. Morphological study of root surfaces in teeth with adult periodontitis. *J Periodontol* 1999;70(11):1283–91. Nov.
- [40] López NJ, Giquoux C, Canales ML. Histological differences between teeth with adult periodontitis and prepubertal periodontitis. *J Periodontol* 1990;61(2):87–94. Feb.
- [41] Philip MP. Periodontal disease and diabetes. *J Dent* 2009;37:s567–84.
- [42] Thrailkill K, Liu L, Wahl E, Bunn R, Perrien D, Cockrell G, et al. Bone formation is impaired in a model of type 1 diabetes. *Diabetes* 2005;54:2875–81.
- [43] Hideki F, Yasuhiro H, Masafumi F. Bone formation in spontaneously diabetic Torii-newly established model of non-obese type 2 diabetes rats. *Bone* 2008;42:372–9.
- [44] Teng YT. The role of acquired immunity and periodontal disease progression. *Crit Rev Oral Biol Med* 2003;14:237–52.
- [45] Olszewska BB, Burakowska AK, Węgrzyn G, Banecka JJ. Prevalence of polymorphisms in OPG, RANKL and RANK as potential markers for Charcot arthropathy development. *Sci Rep* 2017;7:501.
- [46] Duarte V, Ramos A, Rezende L, Macedo U, Brandao NJ, Almeida M, et al. Osteopenia: a bone disorder associated with diabetes mellitus. *J Bone Miner Metabol* 2005;23:58–68.